Available online at www.sciencedirect.com

ScienceDirect

Geochimica et Cosmochimica Acta 123 (2013) 166–180

Geochimica et Cosmochimica Acta

www.elsevier.com/locate/gca

Contrasting geochemical cycling of hafnium and neodymium in the central Baltic Sea

Tian-Yu Chen [a,*], Roland Stumpf [a,1], Martin Frank [a], Jacek Bełdowski [b], Michael Staubwasser [c]

[a] GEOMAR Helmholtz Centre for Ocean Research Kiel, Wischhofstraße 1-3, 24148 Kiel, Germany
[b] IOPAN, Institute of Oceanology of Polish Academy of Sciences, P.O. Box 148, Powstańców Warszawy 55, 81-712 Sopot, Poland
[c] Institute of Geology and Mineralogy, University of Cologne, Greinstrasse 4–6, Building 902, 50939 Köln, Germany

Received 19 April 2013; accepted in revised form 9 September 2013; Available online 21 September 2013

Abstract

The central Baltic Sea is a marginal brackish basin which comprises anoxic bottom waters and is surrounded by geological source terrains with a wide variety of compositions and ages. This allows the investigation of water mass mixing using radiogenic isotope compositions of Nd and Hf as well as their geochemical cycling across varying redox conditions in the water column. In this study, we present the distribution of Nd and Hf concentrations and their isotopic compositions for 6 depth profiles and 3 surface water sites obtained during a cruise in the central Baltic Sea onboard the RV Oceania as a part of the international GEOTRACES program.

The results obtained indicate that Nd isotopes effectively trace the mixing between more radiogenic saline waters from the south and unradiogenic fresh waters from the north, which helps to understand the reliability of Nd isotopes as water mass tracer in the open ocean. In surface waters, Nd shows higher concentrations and less radiogenic isotope compositions at the northern stations, which are progressively diluted and become more radiogenic to the south, consistent with the counterclockwise circulation pattern of central Baltic Sea surface waters. In contrast to the variable Nd concentrations, Hf shows much less variability. At the Gotland Deep station, the Nd concentrations of the euxinic waters are higher by a factor >10 than those of the overlying oxygen-depleted waters, whereas Hf only shows small concentration variations. This indicates faster removal of Hf from the water column than Nd. Moreover, the dissolved Hf isotope signatures document great variability but no consistent mixing trends. Our explanation is that Hf has a lower residence time than Nd, and also that the Hf isotope signatures of the sources are highly heterogeneous, which is attributed to their differing magmatic and tectonic histories as well as incongruent post-glacial weathering around the central Baltic Sea.

1. INTRODUCTION

Combined Nd and Hf isotope compositions of seawater have been used for tracing present and past ocean circulation, as well as continental weathering inputs (e.g., Lee et al., 1999; Piotrowski et al., 2000; David et al., 2001; van de Flierdt et al., 2002). With a mean oceanic residence time of several hundred years (Arsouze et al., 2009; Rempfer et al., 2011), Nd is considered a quasi-conservative tracer for water mass mixing (e.g. von Blanckenburg, 1999; Frank, 2002; Goldstein et al., 2003). Seawater Nd is supplied via boundary exchange with shelf sediments (Amakawa et al., 2000; Lacan and Jeandel, 2001, 2005; Tachikawa et al., 2003), dust dissolution and riverine inputs, whereas hydrothermal contributions have been suggested to be negligible (German et al., 1990; Halliday et al., 1992). In the oceanic water column, Nd undergoes reversible scavenging

* Corresponding author. Tel.: +49 04316002251.
E-mail address: tchen@geomar.de (T.-Y. Chen).
[1] Now at Department of Earth Science & Engineering, Imperial College London, London SW7 2AZ, UK.

0016-7037/$ - see front matter © 2013 Elsevier Ltd. All rights reserved.
http://dx.doi.org/10.1016/j.gca.2013.09.011

by particles (Bertram and Elderfield, 1993; Sholkovitz et al., 1994; Nozaki and Alibo, 2003) resulting in a progressive increase in dissolved Nd concentrations with depth (Siddall et al., 2008; Arsouze et al., 2009; Oka et al., 2009; Rempfer et al., 2011). In contrast, the marine geochemistry of Hf is much less well constrained, and only a few Hf isotopic data for dissolved continental inputs are available (Bayon et al., 2006; Godfrey et al., 2009; Zimmermann et al., 2009a; Rickli et al., 2013). Estimates of the present day mean residence time of Hf in the global ocean range from a few hundred years (comparable to or shorter than that of Nd) to several thousand years (and thus longer than the global ocean mixing time) (Godfrey et al., 1996, 2008, 2009; Rickli et al., 2009, 2010; Zimmermann et al., 2009a,b; Firdaus et al., 2011). Moreover, Hf cycling in the water column is also poorly understood. Open ocean Hf has been reported to have slightly higher concentrations in deep waters than in the surface mixed layer (Rickli et al., 2009; Zimmermann et al., 2009b; Stichel et al., 2012a), indicating that Hf experiences biogeochemical cycling similar to Nd. However, a previous study also hypothesized that Hf in seawater may be dominantly associated with colloidal Fe oxides rather than Mn oxides or truly dissolved species ($Hf(OH)_5^{-1}$) (Byrne, 2002). In contrast, dissolved Nd speciation in the open ocean is dominated by $NdCO_3^+$, $Nd(CO_3)_2^-$, and a fraction bound to colloids (both negatively and positively charged, Byrne, 2002; Dahlqvist et al., 2005; Bau and Koschinsky, 2006).

The central Baltic Sea is a strongly stratified shallow brackish basin with a number of areas where bottom waters are permanently anoxic (e.g., Hansson et al., 2009), and where intense cycling of organic material and redox sensitive elements such as Fe and Mn occurs. Since the sink of both Nd and Hf from seawater is most likely closely related to Fe/Mn hydroxides and organic species (e.g., Ingri et al., 2000; Bau and Koschinsky, 2006), the central Baltic Sea is ideal to investigate Nd–Hf geochemical cycling in the water column. In addition, as a semi-enclosed basin dominated by continental inputs (i.e., no hydrothermal contributions), combined dissolved Nd–Hf isotope compositions from the Baltic Sea provide direct weathering signatures from the continent and will thus contribute to the understanding of how the seawater Nd–Hf isotope relation (e.g., Albarède et al., 1998) is generated.

In an early study (with one reported station in the central Baltic Sea), Andersson et al. (1992) showed that Nd isotopes in the Gulf of Bothnia are significantly less radiogenic than Atlantic-derived waters from the southern Baltic Sea. In addition, Nd concentrations were found to be enriched in anoxic bottom waters, consistent with other studies on REE distributions in anoxic water bodies (e.g., German et al., 1991). In this study, we analyzed the Hf and Nd isotopic compositions and concentrations of 6 depth profiles and 3 surface sites in the central Baltic Sea (Fig. 1). In particular, a high resolution profile (20–30 m sampling interval across the redoxcline) in the Gotland Deep is presented to investigate Nd and Hf cycling at the oxic–anoxic interface. These data represent the first systematic investigation of the distribution of combined Hf–Nd concentrations and isotope compositions in a marginal periodically anoxic ocean basin.

2. HYDROGRAPHIC AND GEOLOGICAL BACKGROUND

The semi-enclosed central Baltic Sea is characterized by salinities ranging between 5 and 8 at the surface and 10 and 14 in bottom waters (mostly shallower than 250 m), with a counterclockwise circulation (Fig. 1) (Meier, 2007). It is one of the largest brackish water bodies on Earth. Saline and dense inflow from the Atlantic (about 16,100 m^3/s) spills over the shallow sills of the Kattegat and then largely transforms into bottom waters when it enters the central Baltic Sea (Meier, 2007; Reissmann et al., 2009). Freshwater is supplied by rivers and precipitation to the surface mixed layer. This estuarine circulation system promotes stable stratification of the water column and widespread anoxia in bottom waters (e.g., Hansson et al., 2009; Reissmann et al., 2009). In the central Baltic Sea, the halocline is at 40–80 m depth, coinciding with a sharp decrease in oxygen content. The ventilation of the major central Baltic anoxic bottom water bodies (i.e. the Gotland Deep, the Landsort Deep) only occurs episodically, via strong and fast intrusions of oxygen-rich and saline North Sea-derived water, i.e. once per several years. The latest major ventilation event occurred in 2003 (Feistel et al., 2003). Northward advection of saline deep water into the Gulf of Bothnia is prevented by a sill between the central Baltic Sea and the Aland Sea, resulting in the restriction of water mass exchange between these two basins.

The modern catchment area of the Baltic Sea (Fig. 1) includes a wide range of geological source terrains from Cenozoic sedimentary rocks in the south to the very old Proterozoic and Archean rocks of northern Scandinavia (e.g., Gaál and Gorbatschev, 1987; Mansfeld, 2001; Kuhlmann et al., 2004; Bock et al., 2005). The rivers that drain the Paleozoic, Proterozoic, and Archean terrains mostly flow into the Gulf of Bothnia or the Gulf of Finland, while rivers draining younger terrains are restricted to the southern Baltic Sea (Fig. 1). Neodymium and hafnium concentrations as well as isotope compositions of two rivers (Schwentine and Kalix) were measured for reference in this study. The Schwentine river is a small river in northern Germany with a length of only about 62 km. Its catchment area (Schwentine basin) is part of the lowlands of northern Germany, which have been affected by the active land-based Scandinavian glaciers during the Middle and Late Pleistocene (Piotrowski, 1997). The topmost layer of the Schwentine basin consists of sediments deposited during the Holocene and the last glacial stage, while the unconsolidated subsurface layers largely consist of glaciolacustrine or lacustrine sands and clays deposited during earlier glacial stages (e.g., Marine Isotope Stages 6 and 12, Piotrowski, 1997). In contrast, the major part of the basement of the Kalix river system consists of Precambrian intermediate and basic volcanic rocks and granitoids (Gaál and Gorbatschev, 1987). However, bedrock exposure represents less than 1% of this area, which is mainly covered by coniferous forests and peatlands. The soils are dominated by podsols developed on tills, which likely formed after the retreat of the last glaciers from this area during the early Holocene (i.e., around 9 ky before present, Lundqvist, 1986).

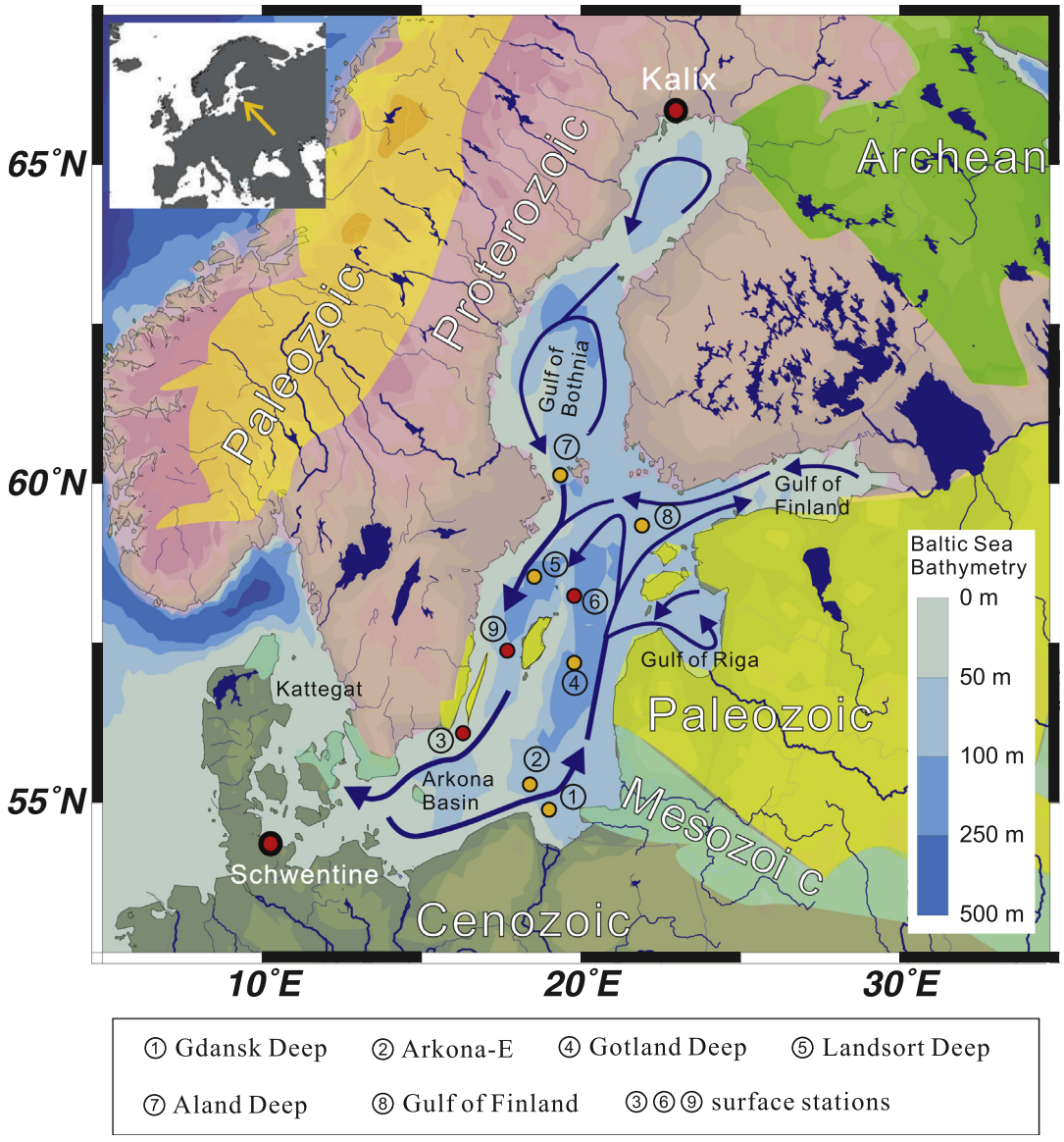

Fig. 1. Map illustrating the sampling locations of the GEOTRACES cruise on R/V Oceania in the central Baltic Sea in November 2011, as well as the river water sampling locations (generated using Ocean Data View, Schlitzer, 2012). Red dots represent surface water stations whereas yellow dots represent depth profile stations. Also shown is the simplified geology of the continental area surrounding the Baltic Sea (after Kuhlmann et al., 2004). (For interpretation of the references to color in this figure legend, the reader is referred to the web version of this article.)

3. SAMPLING AND METHODS

Water samples were collected in the central Baltic Sea at 6 depth profiles and 3 surface water sites during the GEOTRACES cruise on RV Oceania in November 2011. Stichel et al. (2012a,b) provided a detailed description of the sampling procedures, REE/Hf pre-concentration, chromatography, and mass spectrometric measurements. We will therefore describe these only briefly here given that we basically followed the same protocols in the same laboratory at GEOMAR, Kiel, procedures that are identical to the agreed GEOTRACES protocols (http://www.obs-vlfr.fr/GEOTRACES/libraries/documents/Intercalibration/Cookbook.pdf). Sixty liters of seawater were sampled using 3 acid-cleaned 20 L LDPE-collapsible cubitainers for each sample. The deep and surface water samples were taken from a standard rosette equipped with Niskin bottles and a surface pump, respectively. Immediately after collection, samples were filtered through 0.45 μm nitro-cellulose acetate filters. The two river water samples were taken from the Kalix river, Sweden, in June 2012 and the Schwentine river, Germany in July 2012. Both samples were very rich in particles. The Kalix river is characterized by low concentrations of suspended detrital particles but relatively high

concentrations of organic and Fe-oxyhydroxide particles (Ingri et al., 2000). While the Schwentine sample was filtered immediately, the filtration of Kalix river water was delayed for about two months after collection. Thus, the measured concentrations are likely to be lower than directly after sampling due to adsorption processes. After filtration, all the samples were acidified to pH = ~2 using distilled, concentrated HCl. For precise laboratory-based concentration measurements of Hf and Nd, 2 L aliquots of the filtered and acidified samples were kept separately in clean PE-bottles. The hafnium and neodymium in large volume seawater samples for isotopic measurement were pre-concentrated on board by co-precipitation with Fe-hydroxide (see details in Stichel et al., 2012a) at a pH of 8–9 through addition of super-pure ammonia.

To further reduce the amount of major elements (e.g., Mg), the precipitates for the isotope measurement were re-dissolved and precipitated at lower pH (7–8) prior to element purification in the laboratory. The precipitates were then centrifuged and rinsed with deionised water (MilliQ system), and finally transferred into Teflon vials. Subsequently, the samples were treated with aqua regia to destroy organic matter and were then dissolved in 6 M HCl. A back extraction method using a diethyl ether phase was applied to remove the large amounts of Fe while keeping Hf and Nd dissolved in an acidic phase. Hafnium and Nd were then separated and purified following the established methods of Stichel et al. (2012a,b). Procedural blanks for Nd and Hf isotopes were less than 1% of the sample amounts.

For Hf and Nd concentration analyses, about 0.5 L of water was taken from the 2 L aliquot samples. Pre-weighed ^{178}Hf single spike and ^{150}Nd spike solutions were added to each sample (e.g., Rickli et al., 2009). After 4–5 days of isotopic equilibration, the samples were co-precipitated with Fe-hydroxide at pH 7–8. Further separation of Hf and Nd was carried out by cation chromatography (1.4 ml resin bed, BIORAD® AG50W-X8, 200–400 mesh-size). Duplicate samples of Nd concentrations in subsurface water were processed about one month later than the first batch of measurements, and yielded an external reproducibility of better than 1%. Due to the limited amount of Hf spike available in our laboratory, no duplicate samples for Hf concentrations were analyzed. The reproducibility of Hf concentration measurements reported by Stichel et al. (2012a,b) from the same laboratory was 3–10% depending on concentrations. Procedural blanks for concentration measurements were 14–23 pg for Nd and 6–8 pg for Hf ($n = 2$), which has been applied to the sample concentration corrections.

Hafnium and neodymium isotope ratios were measured on a Nu instruments MC-ICP-MS at GEOMAR, Kiel. Instrumental mass bias was corrected using a ^{146}Nd/^{144}Nd ratio of 0.7219 and a ^{179}Hf/^{177}Hf ratio of 0.7325, applying an exponential mass fractionation law. Concentrations of the Nd and Hf standards measured during each session were adjusted to be similar to those of the samples. All ^{176}Hf/^{177}Hf results were normalized to JMC475 = 0.282160 (Nowell et al., 1998) while all ^{143}Nd/^{144}Nd results were normalized to JNdi-1 = 0.512115 (Tanaka et al., 2000). The 2σ external reproducibility deduced from repeated measurements of the Hf and Nd isotope standards at concentrations similar to those of the samples was ±1.30 and ±0.30 epsilon units, respectively. Some seawater samples still contained a considerable amount of Yb (i.e., up to 1.98% contribution on mass 176), which cannot be adequately corrected by applying the exponential mass fractionation factor derived from ^{179}Hf/^{177}Hf and the commonly accepted Yb isotope ratios (Chu et al., 2002). Therefore, we adopted a Yb-doped JMC475 standard calibration method for all of the seawater samples, in order to precisely correct the Yb contribution (Stichel et al., 2012a). The extra corrections (i.e., after the standard internal mass fractionation correction using ^{179}Hf/^{177}Hf) to the seawater samples based on Yb-doping never exceeds 3.2 ε_{Hf} units. Given that the variation in the Hf isotope compositions of the differently doped JMC475 standards were linearly correlated ($R^2 = 0.97$) with the Yb contribution, this additional correction method is considered to provide reliable results.

4. RESULTS

4.1. Hydrography and concentrations of Hf and Nd

The hydrographic data of the 6 studied depth profiles obtained during the RV Oceania cruise are presented in Fig. 2. The cold temperatures near 50 m water depth (Fig. 2a) correspond to the seasonal thermoclines (stations 1, 2, 4, 5) which are shallower than the corresponding haloclines (Fig. 2b). From south to north (Fig. 1), deep water salinities become progressively lower (Fig. 2b). The rapid decreases in oxygen concentrations observed at the other depth profiles roughly coincide with the haloclines, the only exception being the Aland Deep where strong vertical mixing prevails (Fig. 2b and c).

Due to the lack of sulfide concentration data from our cruise, it is difficult to define the exact depth of euxinia for each depth profile, despite the fact that widespread euxinia have been reported in bottom waters of the central Baltic Sea during periods of prolonged stagnation (Matthäus et al., 2008). In addition, we only have 2 or 3 samples for most of the depth profiles (except the Gotland Deep). Any further subdivision of the anoxic layers has thus not been attempted for most stations and would also not substantially contribute to the results of our study. Only the anoxic waters of the Gotland Deep profile (where high resolution sampling was performed) will be further divided into an "oxygen-depleted" layer and a "euxinic" layer (see Section 5.3.1 for details).

Hafnium and neodymium concentration data obtained in the central Baltic Sea are shown in Table 1 and Fig. 3. Overall, Nd concentrations in surface water (upper 5 m water depth) of stations 1–4 are slightly lower than those of stations 5–9, Table 1), with a total range from 14.6–34.6 pmol/kg. The maximum surface concentration is observed at Aland Deep (station 7), and the minimum is found at Gdansk Deep (station 1). Except for the Aland Deep (station 7) and Arkona-E (station 2), the other 5 depth profiles (Fig. 3) reveal a general increase in Nd concentrations with depth. In particular, Nd concentrations reach a maximum value of 150 pmol/kg in Gotland Deep

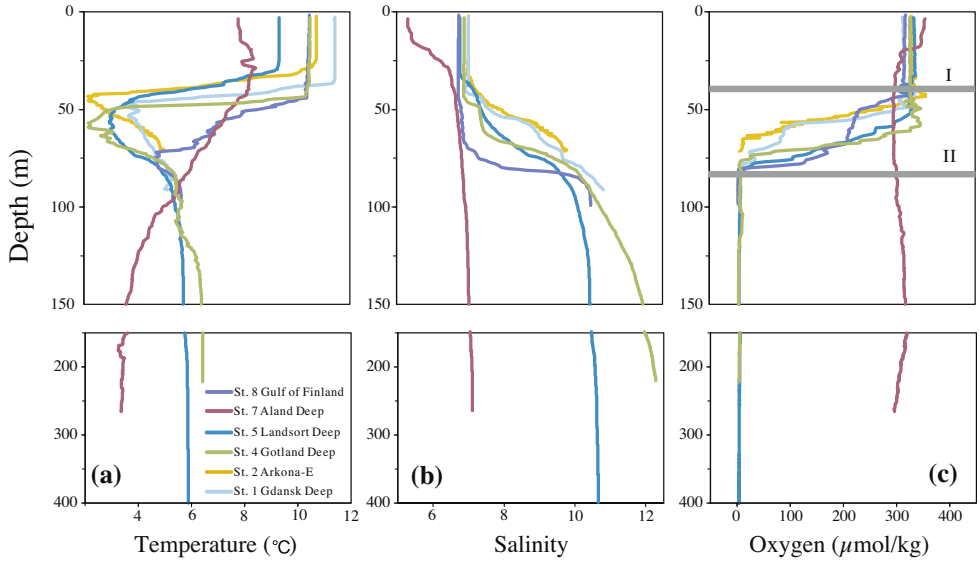

Fig. 2. Temperature (a), salinity (b), and oxygen concentration (c) of the studied depth profiles. (I): boundary between the mixed layer and the subsurface halocline layer (~40 m water depth); (II) boundary between the subsurface halocline layer and the anoxic layer (~80 m water depth).

bottom waters, while the bottom water sample of the Landsort Deep is only moderately enriched in Nd (48.6 pmol/kg). Neodymium enrichments are also observed in bottom waters of the Gulf of Finland (station 8) and the Gdansk Deep (station 1) at a shallower depth (~90–100 m). Moreover, surface Hf concentrations at station 5, 7, and 8 are distinctly higher than the other stations, while the Hf concentrations in the halocline layer are generally lower than in the corresponding surface water. In contrast to a total range of Nd concentrations of 14.6 to 150.5 pmol/kg in the central Baltic Sea, Hf concentrations show a significantly smaller variability (0.6–1.7 pmol/kg). While a slight increase in Hf concentration is observed in the Gotland Deep profile (from 1.0 pmol/kg at the surface to 1.5 pmol/kg at 160 m depth), Hf concentrations decreased slightly in bottom waters of Gulf of Finland (from 1.6 at the surface to 1.3 pmol/kg) and of the Landsort Deep (from 1.8 at the surface to 0.9 pmol/kg).

4.2. Distribution of Hf and Nd isotope compositions

Both Nd and Hf show large isotopic variability in surface waters (Fig. 3). The Nd isotope compositions become systematically less radiogenic from the Gdansk Deep ($\varepsilon_{Nd} = -14.4$) to the Aland Deep ($\varepsilon_{Nd} = -17.1$) along the counterclockwise pathway of the surface currents. The return flow along the southeastern coast of Sweden becomes more radiogenic towards the south ($\varepsilon_{Nd} = -16.0$, -15.6) but remains less radiogenic than the eastern part of the central Baltic Sea. In contrast, the Hf isotope compositions of the surface waters display a large range, from $\varepsilon_{Hf} = -5.2$ to $+4.2$ and do not exhibit any clear systematic variations.

In most water column profiles the Nd isotope compositions become progressively more radiogenic with depth (Fig. 3a). The only exception is the Aland Deep station, which shows invariant Nd isotope signatures. No abrupt changes in Nd isotope compositions are observed at the oxic–anoxic interfaces at the sampled depth resolutions (Fig. 2, Fig. 3a). In contrast to the Nd isotope distributions, there are less consistent trends in the Hf isotope profiles (Fig. 3b). In the Aland Deep, Hf isotope composition becomes less radiogenic with depth (ε_{Hf} +1.2 to −6.9 between 5 and 260 m depth), while Nd isotope compositions are homogeneous (ε_{Nd} around −17.0). Except for the stations at the Gdansk Deep and in the Gulf of Finland which remain constant with depth in ε_{Hf}, all other stations show a shift to less radiogenic ε_{Hf} signatures in the same depth range between 5 and 80 m. Unlike the profiles in the Aland and Landsort Deeps, which document a continuous trend to less radiogenic ε_{Hf} signatures towards the bottom of the profiles, the high resolution profile of Gotland Deep reveals an abrupt shift in Hf isotope compositions back to a more radiogenic ε_{Hf} signatures of +1.3 at 110 m depth, followed by a sharp negative shift to −2.7 at 130 m. Below 130 m, the Hf isotope compositions stays invariant.

4.3. Kalix and Schwentine river

Hafnium concentrations in river waters (Kalix: 12.9 pmol/kg, Schwentine: 6.4 pmol/kg) are notably higher than those of Baltic seawater (0.6–1.7 pmol/kg) and are in the same range as previously reported concentrations in Arctic rivers (7.6–29.6 pmol/kg, Zimmermann et al., 2009a), but are higher than those reported for Alpine rivers (0.05–5.3 pmol/kg, Rickli et al., 2013). The ε_{Hf} (+15.0)/ε_{Nd} (−25.4) signatures of the Kalix river sample are exceptionally radiogenic/unradiogenic compared to Baltic seawater samples, while its Nd isotope composition agrees well with earlier observations during summer months (−24.8 to −26.5 from May to June, Andersson et al., 2001). In contrast, the Hf isotope composition of the Schwentine river is particularly unradiogenic ($\varepsilon_{Hf} = -10.7$), while its Nd

Table 1
Hf and Nd concentrations and isotope compositions of samples from the central Baltic Sea and rivers.

Station No.[a]	Latitude (N)	Longitude (E)	Depth (m)	T (°C)	S	Hf (pmol/kg)	Nd (pmol/kg)	ε_{Nd}[b]	Int. (±1 SEM)	ε_{Hf}[c]	Int. (±1 SEM)
Central Baltic Sea											
1	54°55′	18°59′	5	11.44	7.04	0.9	14.6	−14.4	±0.08	−3.0	±0.35
1	55°01′	18°59′	90	5.09	10.79	1.4	69.5	−13.5	±0.08	−3.3	±0.35
2	55°19′	18°25′	5	10.75	7.03	1.0	18.5	−15.4	±0.06	3.9	±0.46
2	55°22′	18°22′	80	5.03	9.81	0.6	19.4	−14.3	±0.08	−2.0	±0.42
							19.4[d]				
3	56°06′	16°19′	5			1.0	20.8	−15.6	±0.08	0.8	±0.39
4	57°11′	19°47′	5	10.51	6.91	1.0	23.1	−15.2	±0.10	−0.3	±0.46
4	57°14′	19°59′	80	5.29	9.99	0.9	21.1	−14.3	±0.12	−6.4	±0.74
							21.0[d]				
4	57°14′	19°59′	110	5.68	11.09	0.8	11.9	−13.9	±0.12	1.0	±0.35
							11.9[d]				
4	57°15′	19°55′	130	6.28	11.64	0.9	31.2	−14.1	±0.10	−3.0	±0.35
							31.3[d]				
4	57°15′	19°54′	160	6.43	12.04	1.5	102.0	−13.6	±0.16	−2.5	±0.32
							102.5[d]				
4	57°15′	19°57′	220	6.43	12.28	1.4	150.5	−13.1	±0.35	−2.2	±0.42
							151.0[d]				
5	58°39′	18°24′	60	3.38	8.11	1.2	22.7	−15.3	±0.08	−6.5	±0.28
							22.7[d]				
5	58°40′	18°23′	344	5.88	10.66	0.8	48.6	−14.5	±0.12	−9.1	±0.46
							48.9[d]				
5	58°33′	18°33′	5	9.44	6.79	1.6	23.5	−16.0	±0.12	−4.2	±0.32
6	58°16′	19°46′	5	10.06	6.79	1.1	21.8	−15.3	±0.10	−2.4	±0.35
7	60°05′	19°17′	5	7.99	5.64	1.7	34.6	−17.1	±0.10	0.9	±0.21
7	60°06′	19°21′	60	5.22	6.95	1.3	29.0	−16.8	±0.10	−4.7	±0.28
7	60°08′	19°16′	260	3.37	7.11	1.5	28.1	−16.9	±0.10	−7.2	±0.32
							28.1[d]				
8	59°22′	21°56′	5	10.48	6.75	1.7	21.7	−16.3	±0.12	−5.6	±0.28
8	59°22′	21°59′	98	5.67	10.48	1.3	60.7	−14.7	±0.12	−5.7	±0.28
							60.6[d]				
9	57°24′	17°43′	5			1.1	26.6			−1.1	±0.35
							26.6[d]				
River water											
Kalix			1			12.9	575.5	−25.1	±0.08	16.6	±0.18
Kalix-duplicate sample			1					−25.4	±0.08	15.0	±0.18
Schwentine			1			6.4	17.8	−13.8	±0.10	−10.7	±0.35

[a] Referring to Fig. 1.
[b] $\varepsilon_{Nd} = [(^{143}Nd/^{144}Nd)_{sample}/(^{143}Nd/^{144}Nd)_{CHUR} - 1] * 10^4$; where $(^{143}Nd/^{144}Nd)_{CHUR} = 0.512638$ (Jacobsen and Wasserburg, 1980).
[c] $\varepsilon_{Hf} = [(^{176}Hf/^{177}Hf)_{sample}/(^{176}Hf/^{177}Hf_{CHUR}) - 1] * 10^4$; where $(^{176}Hf/^{177}Hf)_{CHUR} = 0.282769$ (Nowell et al., 1998).
[d] Duplicate sample for Nd concentration measurement.

isotope composition ($\varepsilon_{Nd} = -13.8$) is close to that of the southern Baltic surface waters (e.g., Gdansk Deep, −14.4).

5. DISCUSSION

5.1. Processes controlling Hf and Nd isotope compositions of surface waters

Freshwater inputs to the Baltic Sea are dominated by river discharge. About 80% of the continental runoff originates from catchment areas around the Gulf of Bothnia, the Gulf of Finland, and the Gulf of Riga (Fig. 1, Graham, 2000), thus controlling the north–south surface water salinity gradient of the central Baltic Sea. Correspondingly, the surface waters at the location of the Aland Deep are the freshest of our dataset (5.64 psu) and show the highest Nd and Hf concentrations (Fig. 3b and d), which is consistent with the high Hf and Nd concentrations observed in the Kalix River. The unradiogenic Nd isotope signature at this location is due to weathering inputs from the Precambrian basement rocks of the northern terrains, which is supported by the low ε_{Nd} of the Kalix river sample. Towards the south, Nd concentrations linearly decrease with increasing salinity (Fig. 4), accompanied by more radiogenic Nd isotope signatures. The processes controlling the Nd isotope compositions in the surface ocean of the southern Baltic Sea are complicated by strong vertical mixing (e.g., at Arkona Basin, Meier, 2007; Reissmann et al.,

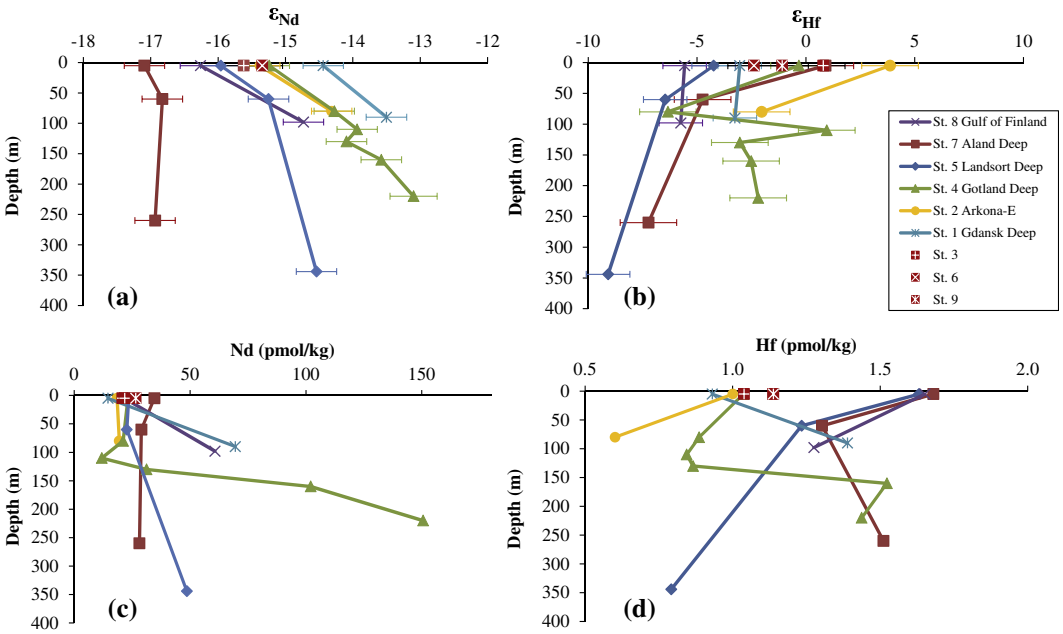

Fig. 3. Neodymium and hafnium isotope compositions (a and b) and concentrations (c and d), respectively, as a function of water depth in the central Baltic Sea.

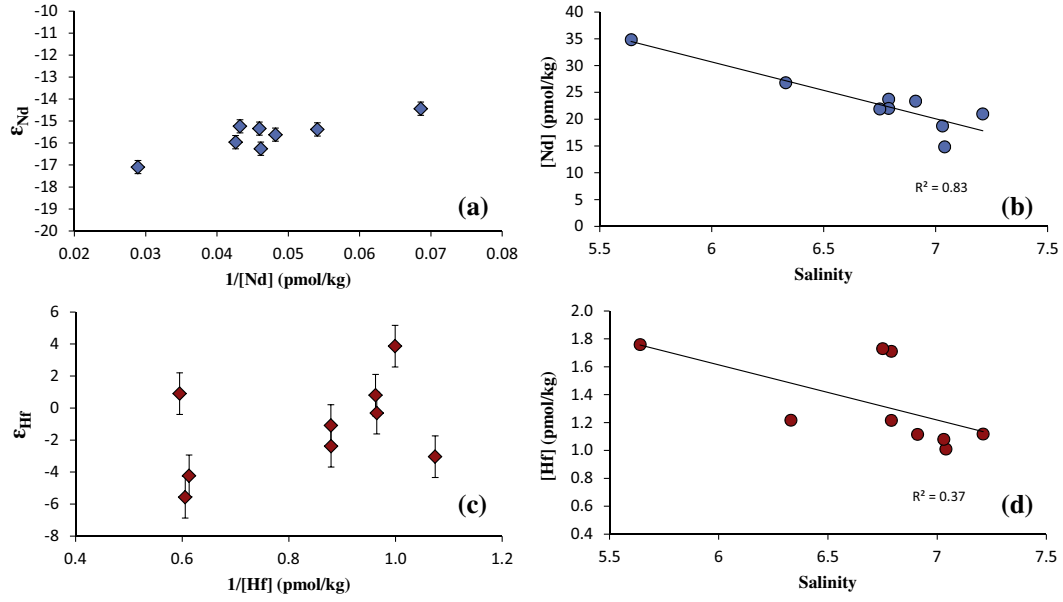

Fig. 4. Neodymium and hafnium relationships in surface waters. (a) ε_{Nd} versus reciprocal Nd concentrations, (b) Nd concentrations versus salinity, (c) ε_{Hf} versus reciprocal Hf concentrations, (d) Hf concentrations versus salinity. Solid lines represent linear regressions of the concentration data.

2009) and weathering contributions supplied from different southern source terrains (e.g., Cenozoic-Mesozoic sedimentary or volcanic rocks). Nevertheless, the central Baltic surface Nd concentration and isotope data are well explained by quasi-conservative mixing between southern and northern source waters, as demonstrated by the correlations between ε_{Nd} and 1/[Nd], as well as of Nd concentration and salinity (Fig. 4a and b). This implies that Nd inputs to the central Baltic surface waters can be grouped into two distinct sources: the old and unradiogenic source rocks in the north and the young and radiogenic ones in the south (including both local weathering inputs and supply of Atlantic water), consistent with the geological framework presented in Fig. 1. In addition, considering the close asso-

ciation of surface water Nd isotope variations with the natural source inputs, anthropogenic contamination should have negligible influence on the geochemical cycling of Nd in the central Baltic Sea.

In contrast to Nd, the scatter of the Hf concentrations and isotopic compositions compared to salinity (Fig. 3c and d) confirms the heterogeneous distribution of Hf isotope compositions in central Baltic Sea surface waters, excluding a simple binary mixing system comparable to the one observed for Nd. In view of the very large difference in the Hf isotope composition of the Kalix and Schwentine rivers, we suggest that the behavior of Hf in surface waters is most likely caused by highly variable Hf isotope signatures (e.g., due to incongruent weathering) supplied by different rivers, combined with a shorter residence time of Hf than of Nd.

If we extrapolate the Nd concentrations to a salinity of zero (Fig. 4b), a fresh water endmember with a Nd concentration of about 94 pmol/kg is obtained, which is significantly lower than that of the Kalix river water sample (576 pmol/kg). This implies that a large fraction of the fresh water Nd (85% of the Kalix river Nd) is lost in the estuarine system, which is in good agreement with previous observations (e.g., Lawrence and Kamber, 2006). A similar extrapolation in Fig. 4d results in a fresh water endmember Hf concentration of about 4 pmol/kg (30% of the Kalix river Hf concentration). In comparison, Godfrey et al., 2008 reported a ~50% dissolved Hf removal during mixing in the Hudson river estuary. It appears that there is less Hf loss from fresh water during estuarine mixing and/or more reworking and release of Hf from the shelf sediments, and thus a more efficient transfer of local signatures to the Baltic compared with Nd. Nevertheless, we are aware that one single data point from the Kalix River and the poor correlation in Fig. 4d essentially prevent a confident extrapolation of the Hf concentrations. More studies on Hf behavior in estuarine systems are needed before robust conclusions can be drawn.

5.2. Hf and Nd isotope compositions in the halocline layer

At the upper boundary of the halocline layer, oxygen contents start to decrease rapidly but the waters do not become anoxic (Fig. 2). Hafnium concentrations (and to a lesser extent Nd concentrations) exhibit a small decrease from the oxygenated surface layer into the halocline layer (Fig. 5a and b, 40–80 m water depth). Given that the magnitude of concentration decrease has no apparent relationship with the salinity changes from the surface to the halocline (Fig. 2b), it is likely that this decrease is regulated by local scavenging effects besides mixing of the advected water masses.

We assume that surface water Nd isotope compositions reflect the potential isotopic range of local weathering sources ultimately supplied to the subsurface waters. At the four stations where samples of the halocline layer are available (Fig. 5), Nd isotope compositions of the halocline are all more radiogenic, thus indicating that advective supply of Nd must contribute to the observed variability. In this respect, the Nd isotope compositions and hydrographic properties of the halocline layer are consistent with the contribution of more saline and radiogenic Atlantic waters entering the southern Baltic Sea. However, the same scenario does not explain the distribution of Hf isotope compositions because the Atlantic seawater Hf source to the halocline should be characterized by ε_{Hf} signatures near 0 (if Bay of Biscay data can be considered representative, Rickli et al., 2009, 2010). Despite the fact that the subsurface

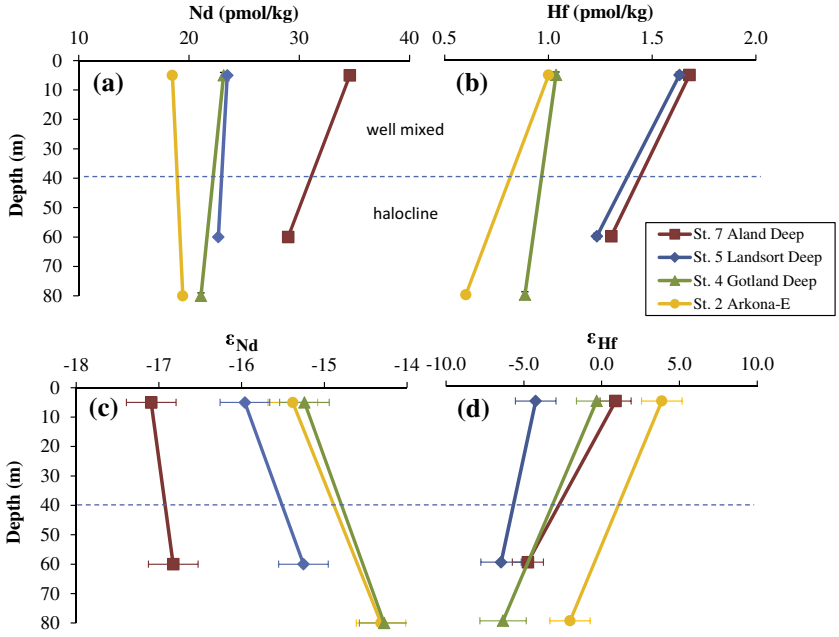

Fig. 5. Comparison between Nd and Hf concentrations (a and b) and isotope compositions (c and d) in surface and subsurface oxygenated waters.

E-Arkona sample can be explained by advective contributions of Atlantic waters, the other halocline samples are too unradiogenic in ε_{Hf} to be consistent with mixing with Atlantic source waters. We thus infer that the halocline decrease in ε_{Hf} represents mixing of Hf from local advective sources, which is not observed for Nd. This supports a shorter residence time for Hf in the water column than Nd (Rickli et al., 2009), which is also in agreement with the heterogeneous distribution of the surface water Hf isotope compositions (Fig. 4c).

5.3. Comparison of Hf and Nd cycling across the redox interface

To better understand the factors controlling Nd and Hf geochemical cycling across the redox transitions, we identify three typical metal concentration profiles observed at the Gotland Deep station (stable, depleted, and enriched; Fig. 6). Firstly, the stable profile represents trace metal concentrations with little variation (i.e., less than a factor of 2). This normally includes the conservative trace elements such as Sr (Andersson et al., 1992), and highly particle reactive elements such as Pb (e.g., Pohl and Hennings, 2005). Secondly, many elements such as Cd, Zn, and Cu, exhibit depleted concentrations in euxinic waters, which is caused by the formation of insoluble sulfide precipitates. However, there may nevertheless be a slight increase in concentration from the surface to the halocline layer due to the decomposition of organic particles and associated metal release (Pohl and Hennings 2005). The third type shows enriched concentrations in the euxinic layer, which includes Fe, Mn (Neretin et al., 2003; Pohl et al., 2004; Staubwasser et al., 2013) and closely related elements such as Co. The enrichment is a consequence of redox cycling with reductive dissolution and accumulation of Mn and Fe oxy-hydroxides (which also carry Co), in the euxinic waters (Pohl and Hennings, 2005, 2008; Staubwasser et al., 2013).

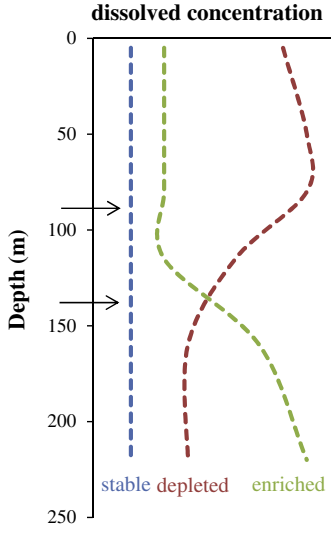

Fig. 6. Schematic illustration of three typical profiles of trace metal concentration variations (stable, depleted and enriched) in the Gotland Deep station (e.g., Pohl and Hennings 2005). The two black arrows indicate the upper and lower boundaries of the oxygen-depleted layer.

5.3.1. Nd cycling

Euxinic conditions have always been found in the Gotland Deep basin during prolonged periods of stagnation similar to the situation prior to our cruise in winter 2011 (e.g., Neretin et al., 2003; Pohl and Fernández-Otero, 2012; Dalsgaard et al., 2013; Staubwasser et al., 2013). Based on NO_3 concentrations obtained on our cruise, anoxic waters of the Gotland Deep are further divided into an oxygen-depleted layer and a euxinic layer (Fig. 7). In the lower part of the oxygen-depleted layer, denitrification leads to a rapid decrease of nitrate concentrations to trace levels, which well defines the approximate depth of the onset of euxinic conditions (e.g., Neretin et al., 2003; Yemenicioglu et al., 2006; Yakushev et al., 2007; Dalsgaard et al., 2013). This is supported by an H_2S concentration profile close to our station obtained on a cruise one year before (August 2010, Fig. 7, Dalsgaard et al., 2013). Neodymium concentrations of the Gotland Deep show a minimum in oxygen-depleted waters followed by a continuous more than an order of magnitude increase with depth in euxinic waters (Fig. 7), consistent with the "enriched profile" revealed in Fig. 6.

Redox cycling of the rare earth elements including Nd was previously studied in detail at other locations (e.g., German et al., 1991; Sholkovitz et al., 1992). It was found that Nd concentration minima generally coincided with maxima in particulate Mn in oxygen-depleted waters, indicating enhanced scavenging of Nd. Below, the reductive dissolution of Mn oxides results in increased concentrations of both dissolved Nd and Mn. Our data are consistent with this observation and support the idea that differences in Nd concentrations between oxygen-depleted and euxinic waters are closely associated with Mn and Fe oxy-hydroxides formation and reductive dissolution.

Throughout the entire water column, Nd isotope compositions become more radiogenic with depth (Fig. 7a), which requires a radiogenic mixing endmember (e.g., the Atlantic waters or release from surface sediments). It is expected that the average Nd isotope composition released from surface sediments should reflect an integrated signature of the anoxic water body at the end of major oxygenation events. Currently, the depth integrated ε_{Nd} of the euxinic water body is about −13.5, which is essentially identical to the bottom boundary layer ($\varepsilon_{Nd} = -13.1$, Fig. 2a). Given a longer period of stagnation, average Nd isotope signatures in the euxinic waters should be even less radiogenic due to the continuous addition of Nd with unradiogenic signatures from the surface waters. Consequently, we conclude that the ε_{Nd} signature of the Nd released from bottom sediment in the Gotland Basin will on average be less radiogenic than −13.5. Thus Atlantic-derived Nd is the most likely candidate for the radiogenic endmember. It is noted that we do not argue against Nd released from dissolution of surface sediments (e.g., Mn-oxides) during anoxia as a potential source to account for the Nd enrichment of the euxinic waters. Rather we suggest that it might not be the radiogenic endmember. For example, if (i) Nd

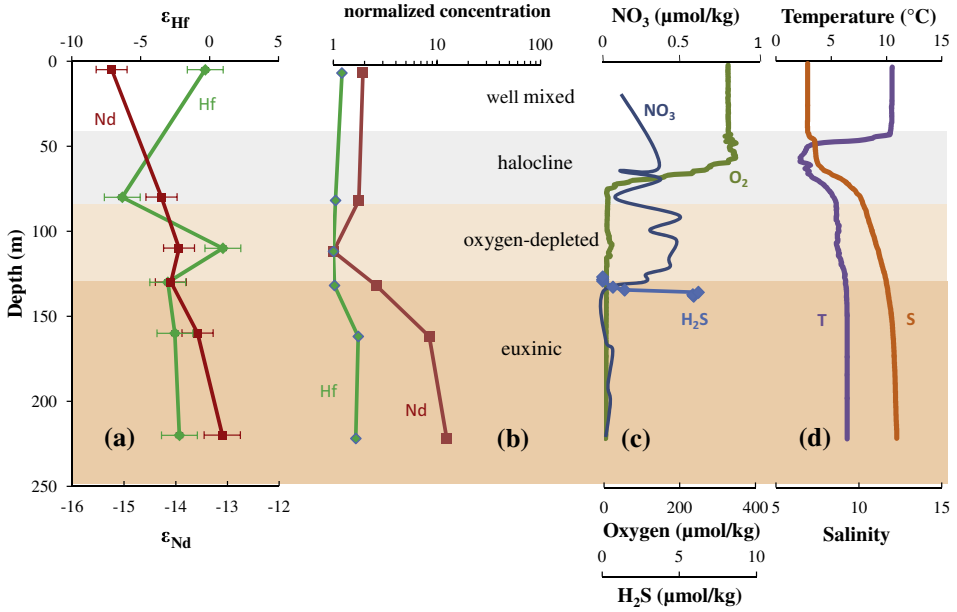

Fig. 7. Vertical profiles of (a) ε_{Hf} and ε_{Nd}, (b) Hf and Nd concentrations (normalized to concentration at 110 m water depth in order to visualize the variability within the oxygen-depleted layer), (c) nitrate, and oxygen concentrations of our cruise, together with H_2S concentrations obtained in 2010 from a profile close to our station (Dalsgaard et al., 2013), (d) temperature and salinity at the Gotland Deep station.

from 110 to 220 m water depth at the Gotland Deep had initial concentrations as low as at the surface (e.g., 21.1 pmol/kg) and initial ε_{Nd} similar to the inflowing signature of the North Sea ($\varepsilon_{Nd} = \sim -10$, Andersson et al., 1992); and (ii) Nd was accumulating in the euxinic water column without being exported to the sediment, mass balance (by summing the Nd concentration × isotope composition for 110 to 220 m water depth) requires an external Nd flux approximately 3 times as high as the initial deep water inventory, with an average ε_{Nd} of about −14.6. This estimated isotope composition is consistent with the subsurface Nd isotope signatures of the Gotland Deep (−14.3). Our result therefore implies that Nd isotope signatures advected with major Atlantic inflow events can still be distinguished after several years of stagnation (i.e., about 8 years).

For a first order approximation, allowing a continuous stagnation (assuming persistent accumulation of Nd in euxinic waters without any removal) in the Gotland Deep and applying the above calculated external flux and ε_{Nd} signature (−14.6), it will require another 8 years for the euxinic waters to reach an ε_{Nd} of about −14.0. Any further decrease of ε_{Nd} will be very slow given that the Nd inventory becomes larger. If the current inventory of Nd has already stabilized in the Gotland Deep euxinic layer (i.e., the sinking flux equals the external inputs), it will only take another 15 years to essentially homogenize the Nd isotopes in the Gotland Deep (i.e., $\varepsilon_{Nd} < -14.3$).

In addition, more than half of the surface water dissolved Nd (<0.45 μm) is probably represented by the fraction bound to colloids in the Baltic (Dahlqvist et al., 2005). Coagulation of these colloids could contribute to the downward flux of Nd to the deep waters. However, this process is most likely of minor importance for the deep enrichment of Nd compared to redox cycling. For example, the Aland Deep shows no enrichment of Nd in the deep water (Fig. 3c), probably due to the lack of redox related Nd cycling.

5.3.2. Hf cycling

The distribution of Hf concentrations and isotope compositions shows no consistent patterns between the different depth profiles. At the Gotland Deep, Hf concentration variations are significantly different from those of Nd (Fig. 7b). A slight increase in Hf concentration only occurs within the euxinic layer. Moreover, the increase of Hf concentrations is not continuous in the euxinic waters. Rather, the concentration at 220 m (1.4 pmol/kg) is essentially the same as at 160 m (1.5 pmol/kg). In the Landsort Deep, we see no enrichment but rather a slight decrease of Hf concentrations in anoxic waters. It is clear, however, that the Hf concentration variability is rather small among all the depth profiles, implying that Hf cycling is not strongly regulated by redox changes.

At the Gotland Deep, the pH is about 8.3 in surface water and decreases to about 7.3 in the euxinic waters (Ulfsbo et al., 2011). In such a pH range, $Hf(OH)_5^{-1}$ is expected to always be the dominant species of "truly dissolved" Hf (Byrne, 2002). On the other hand, given that Hf has very low reduction potential (Plieth, 2008), redox related Hf concentration variations can also be excluded. In fact, the negatively charged $Hf(OH)_5^{-1}$ favors association with slightly positively charged Fe oxyhydroxides (Byrne, 2002; Bau and Koschinsky, 2006). Therefore, Hf concentrations in the water column might be closely associated with Fe cycling. Previous sequential leaching of hydrogenetic Fe–Mn crusts demonstrated that Hf is almost exclusively

associated with the hydrous Fe oxide component (Bau and Koschinsky, 2006). However, it is intriguing that the Hf concentrations increase by a factor of only 1.7 from oxygen-depleted to euxinic waters, while dissolved Fe concentrations increase by up to an order of magnitude in euxinic waters (Turnewitsch and Pohl, 2010). In addition, the Landsort Deep even shows a decrease in Hf concentration of bottom waters. From our data we cannot make a clear judgment whether Hf is exclusively associated with Fe cycling. Other positively charged colloids and particles may also be important but their influence is not clear in this study. Unlike Nd, it is clear that Hf is not strongly affected by Mn redox cycling and is actually close to the "stable concentration profile" introduced above (Fig. 6), thus indicating fast, irreversible removal by particles similar to Pb (Pohl and Hennings, 2005). Schneider et al. (2000) reported a residence time of Pb of only about 0.29 year which may be comparable to the residence time of Hf in the Baltic Sea.

Hf isotope compositions are decoupled from Nd isotope compositions in the Gotland Deep (Fig. 7a). As discussed above, the subsurface minimum in ε_{Hf} (−5.1) probably reflects local lateral supplies rather than from Atlantic waters. The shift of the Hf isotope signature to a value similar to that of the surface layer at 110 m depth is possibly due to the release of surface-derived Hf from dissolution of sinking particles. Alternatively, it may indicate the presence of yet another lateral source. The other depth profiles also do not show clear Hf isotope variations associated with water mass mixing, probably due to the large variability in the Hf isotope signatures of the weathering inputs from different sources and the short residence time in the water column mentioned above.

5.4. Implications for marine Nd and Hf geochemistry

5.4.1. Nd isotopes versus Hf isotopes: the efficiency as water mass tracers in the central Baltic Sea

As shown in Fig. 8, surface water Nd isotope compositions in the central Baltic Sea are in general less radiogenic than in subsurface waters. Thus it may be concluded that more saline subsurface waters reflect larger contribution from the more radiogenic Atlantic waters, as discussed above. Despite the fact that major intrusions of Atlantic waters ($\varepsilon_{Nd} = \sim -10$) only occur sporadically (the last one in 2003), their radiogenic isotope fingerprint is still preserved in the present day anoxic bottom waters of the central Baltic Sea.

Note that the Nd isotopic deviation of the Gdansk Deep surface water sample (southern Baltic) from the overall mixing trend in Fig. 8a still supports the contribution of coastal Southern Baltic Nd input to the surface waters. One interesting question is why the coastal input from the southern Baltic Sea does not appear to be an important mixing endmember for deep waters. Besides the possibility that the sediments from Gulf of Bothnia or Gulf of Finland release Nd more efficiently than the southern Baltic sediments (i.e., supply limitation), we suggest that limitation of the transport of Nd of coastal origin may be important to explain the apparently conservative nature of Nd isotopes (Fig. 8a). On the one hand, inflow from the Atlantic mainly occurs as intrusion events which may experience limited exchange of Nd with the southern Baltic sediments due to the rapidity of the events. On the other hand, abundant fresh water supply from the north and intense vertical mixing (e.g., in the Aland Deep, Fig. 2) could more effectively transport/entrain the unradiogenic Nd into central Baltic deep waters. In contrast, Hf isotope compositions show a heterogeneous behavior and cannot be explained by water mass mixing, i.e. admixture of Atlantic waters (Fig. 8b).

5.4.2. Seawater Nd–Hf isotope array and the impact of weathering on the Hf isotope signatures

Unlike Sm/Nd ratios in different minerals which are generally similar to each other, Lu/Hf ratios vary considerably among different minerals. For example zircon, as a heavy and refractory mineral, hosts much of the Hf in bulk magmatic rocks, resulting in its very low Lu/Hf ratios and unradiogenic Hf isotope compositions (e.g., Patchett et al., 1984; Chen et al., 2011). On the other hand, apatite is highly enriched in rare earth elements (e.g., Lu) but depleted in Hf, and has thus highly radiogenic Hf isotope compositions (e.g., Bayon et al., 2006). It is well known that hydrothermal input is negligible to the seawater Nd budget, while recent studies have also argued against a significant contribution of hydrothermal Hf to seawater (Rickli et al., 2009; Firdaus et al., 2011; Stichel et al., 2012a; Chen et al., 2013).

The data obtained in our study (Fig. 9), although showing large scatter, are significantly more radiogenic in Hf

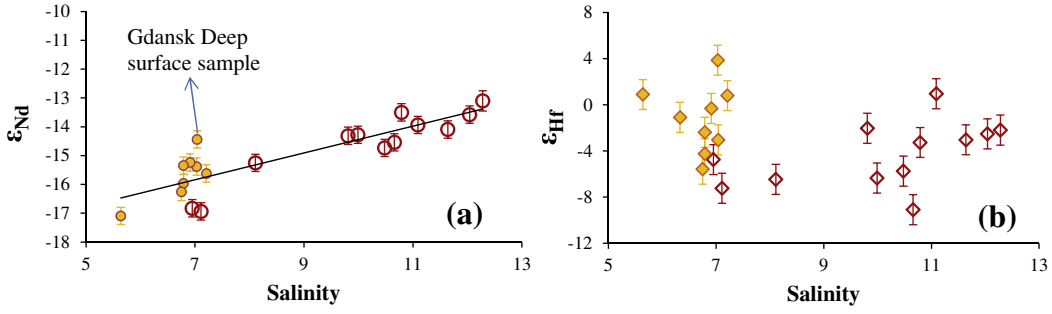

Fig. 8. Neodymium (a) and hafnium (b) isotope compositions versus salinity for all central Baltic Sea water samples. Surface waters are denoted by filled symbols and deep samples are denoted by open symbols.

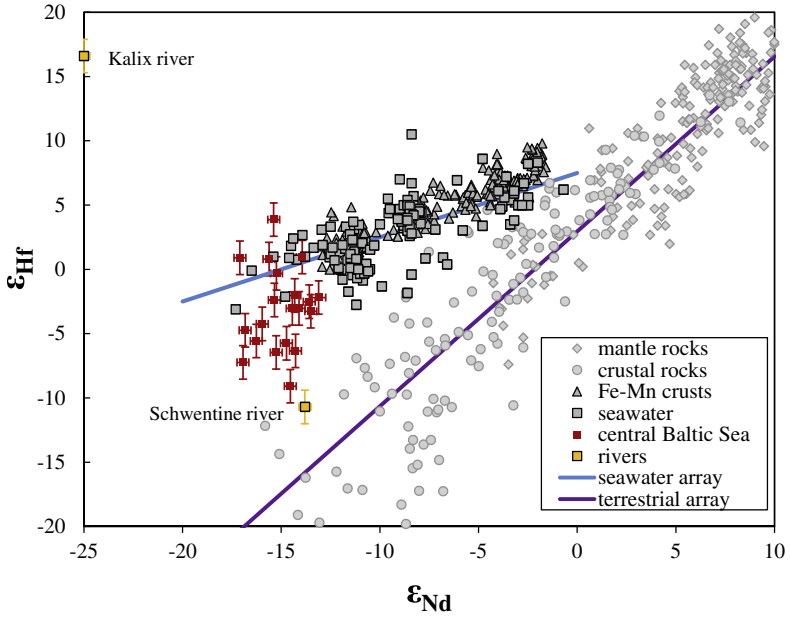

Fig. 9. Neodymium-hafnium isotope systematics of the central Baltic Sea, in comparison with published ε_{Nd}–ε_{Hf} data of terrestrial rocks (terrestrial array, Vervoort et al., 1999), seawater (<0.45 μm, Rickli et al., 2009, 2010; Zimmermann et al., 2009a,b; Stichel et al., 2012a,b) and Fe–Mn crusts (Lee et al., 1999; Piotrowski et al., 2000; David et al., 2001; van de Flierdt et al., 2004; seawater array, Albarède et al., 1998).

isotopes for a given Nd isotope composition compared to terrestrial rocks and are generally consistent with the global seawater Nd–Hf isotope trend. Note that the central Baltic Sea is essentially dominated by continental inputs without hydrothermal influence. Our data thus provide additional support for the suggestion that hydrothermal influence is probably not a significant source for the seawater Hf budget.

During the incipient glacial weathering, trace minerals such as apatite and allanite, which are easily alterable and contain highly radiogenic Hf compositions, are suggested to be preferentially weathered (Bayon et al., 2006). This seems to be supported by Nd–Hf isotope data for the Kalix river (Table 1), which is dominated by input from very recently exposed granitic tills. In fact, because the source rocks of the till are of Archean age (1.8–1.9 Ga, Öhlander et al., 2000), even the Nd isotope compositions have been shown to experience notable incongruent weathering after the early Holocene retreat of the glaciers. For example, the modern ε_{Nd} of the Kalix river (−25.1) is significantly lower than its bulk source materials (−22 ~ −23, Andersson et al., 2001; Öhlander et al., 2000). REE-rich minerals such as allanite and monazite (which are characterized by high Lu/Hf) might be the dominant phases releasing unradiogenic Nd (Andersson et al., 2001; Öhlander et al., 2000) and probably also radiogenic Hf signatures. The Schwentine river, however, shows unexpectedly unradiogenic Hf isotope compositions ($\varepsilon_{Hf} = -10.7$). Rather than an active glacially denuded area like the Kalix river watershed, the Schwentine basin has received sediment deposition from previous glacial cycles, which includes complex sources of different ages with averaged ε_{Nd} around −14 (i.e., the riverine dissolved isotope composition). It is likely that Hf supply to the Schwentine river is dominated by weathering sources which have gone through relatively late magmatic activities and the associated Hf isotope re-equilibrium between different minerals, and thus more similar Hf isotope compositions among different minerals (Chen et al., 2011). Furthermore, the unradiogenic Hf isotope signature of the Schwentine river may also reflect a more congruent weathering signature following the initial radiogenic pulse of Hf. In fact, a radiogenic pulse of Pb and Sr isotope release has been observed during incipient moraine weathering in the field (Blum and Erel, 1997; Harlavan et al., 1998) and for leachates of crushed granitoid samples in lab experiments (Harlavan and Erel, 2002; Erel et al., 2004). These radiogenic isotope signatures are all closely linked with dissolution of easily alterable minerals at the very initial stage of weathering, which may not be the case for the Schwentine catchment.

5.4.3. Oceanic residence time of Hf compared to Nd

Final conclusions on the seawater residence time of Hf and its comparison to that of Nd have not yet been reached (Godfrey et al., 1996; Godfrey et al., 2008, 2009; Rickli et al., 2009, 2010; Zimmermann et al., 2009a,b; Firdaus et al., 2011; Stichel et al., 2012a). In the present day global open ocean, deep water Hf concentrations are not enriched along the deep oceanic conveyor belt, indicating higher particle reactivity of Hf compared to Nd. However, given that the overall global range of seawater Hf concentrations is small, this may also be in agreement with a longer residence time of Hf than that of Nd (Godfrey et al., 2009; Stichel et al., 2012a). The results of our study suggest that Hf is more susceptible to the influence of local sources in the central Baltic Sea. In particular, Hf is not enriched in bottom anoxic waters, indicating fast irreversible particulate removal similar to Pb (Pohl and Hennings, 2005). These

two observations strongly suggest that the oceanic residence time of Hf is likely to be much shorter than that of Nd.

The heterogeneously distributed signatures of dissolved Hf isotope signatures in the Baltic Sea seem to contradict the homogeneity of Hf isotope compositions in the open ocean (Rickli et al., 2009; Zimmermann et al., 2009b; Stichel et al., 2012a). Our preferred interpretation is that: (1) the continental Baltic drainage systems have been under the influence of glacial weathering regimes of very different time scales and lithology (e.g., Lundqvist, 1986), which may result in highly variable degrees of incongruent weathering. Therefore, the central Baltic region is not representative of the global continental source heterogeneity in terms of Hf isotope compositions. (2) Mixing within the source areas, such as reflected by large rivers and eolian dust, effectively erase the large local Hf isotopic variability before entering the open ocean.

6. CONCLUSIONS

The first combined Nd–Hf isotope compositions and concentrations in a marginal brackish basin with anoxic bottom waters (the central Baltic Sea) are presented in this study. While Nd is distinctly enriched in bottom anoxic waters, the overall variability of Hf concentrations is rather small. In a high resolution profile at the Gotland Deep, the different geochemical behavior between Hf and Nd is revealed. We propose that Hf is rapidly removed by particles, which prevents Hf accumulation in anoxic waters, while Nd is closely associated with Mn and Fe redox cycling.

In general, Nd isotope compositions can be explained by quasi-conservative mixing between local inputs and Atlantic-derived more radiogenic subsurface source waters, demonstrating the efficiency of Nd isotope compositions as a water mass tracer in the central Baltic Sea. Hafnium isotope compositions, however, show unexpectedly large variability and the observed patterns are not explainable by water mass mixing. Hafnium is suggested to have a shorter residence time than Nd in seawater, and to be more easily influenced by local inputs. Since the central Baltic Sea is a basin without hydrothermal influence, the general consistency of Hf–Nd isotope data with the global seawater trend implies that continental weathering alone is most likely sufficient to produce the oceanic radiogenic Hf isotope signatures, which is in line with previous studies (Bayon et al., 2009; Rickli et al., 2009; Stichel et al., 2012a; Chen et al., 2013).

ACKNOWLEDGMENTS

Insightful comments from J. Rickli and two other anonymous reviewers greatly improved the manuscript. We also thank our editor D. Vance for the constructive suggestions and polishing the language of the manuscript. We are grateful to the Institute of Oceanology of the Polish Academy of Sciences (IOPAN) at Sopot and the crew of R/V Oceania for their support during the cruise. We thank the scientific steering committee of GEOTRACES who approved this cruise to be a processes study of the GEOTRACES programme and G. Henderson for his invaluable help in planning the cruise. The cruise was prepared as part of the COST action ES0801 of the E.U. We also thank J. Ingri and S. Bauer for providing the Kalix river sample and J. Heinze for the lab support. M. Zieringer provided helpful suggestions about the chemical treatment of seawater Nd–Hf isotope sample. T.-Y. Chen acknowledges financial support from the China Scholarship Council (CSC).

REFERENCES

Albarède F., Simonetti A., Vervoort J. D., Blichert-Toft J. and Abouchami W. (1998) A Hf–Nd isotopic correlation in ferromanganese nodules. *Geophys. Res. Lett.* **25**, 3895–3898.

Amakawa H., Alibo D. S. and Nozaki Y. (2000) Nd isotopic composition and REE pattern in the surface waters of the eastern Indian Ocean and its adjacent seas. *Geochim. Cosmochim. Acta* **64**, 1715–1727.

Andersson P. S., Wasserburg G. J. and Ingri J. (1992) The sources and transport of Sr and Nd isotopes in the Baltic Sea. *Earth Planet. Sci. Lett.* **113**, 459–472.

Andersson P. S., Dahlqvist R., Ingri J. and Gustafsson O. (2001) The isotopic composition of Nd in a boreal river: A reflection of selective weathering and colloidal transport. *Geochim. Cosmochim. Acta* **65**, 521–527.

Arsouze T., Dutay J. C., Lacan F. and Jeandel C. (2009) Reconstructing the Nd oceanic cycle using a coupled dynamical – biogeochemical model. *Biogeosciences* **6**, 2829–2846.

Bau M. and Koschinsky A. (2006) Hafnium and neodymium isotopes in seawater and in ferromanganese crusts: The "element perspective". *Earth Planet. Sci. Lett.* **241**, 952–961.

Bayon G., Vigier N., Burton K. W., Brenot A., Carignan J., Etoubleau J. and Chu N. C. (2006) The control of weathering processes on riverine and seawater hafnium isotope ratios. *Geology* **34**, 433–436.

Bayon G., Burton K. W., Soulet G., Vigier N., Dennielou B., Etoubleau J., Ponzevera E., German C. R. and Nesbitt R. W. (2009) Hf and Nd isotopes in marine sediments: Constraints on global silicate weathering. *Earth Planet. Sci. Lett.* **277**, 318–326.

Bertram C. J. and Elderfield H. (1993) The geochemical balance of the rare-earth elements and neodymium isotopes in the oceans. *Geochim. Cosmochim. Acta* **57**, 1957–1986.

Blum J. D. and Erel Y. (1997) Rb–Sr isotope systematics of a granitic soil chronosequence: The importance of biotite weathering. *Geochim. Cosmochim. Acta* **61**, 3193–3204.

Bock B., Liebetrau V., Eisenhauer A., Frei R. and Leipe T. (2005) Nd isotope signature of Holocene Baltic Mn/Fe precipitates as monitor of climate change during the Little Ice Age. *Geochim. Cosmochim. Acta* **69**, 2253–2263.

Byrne R. H. (2002) Inorganic speciation of dissolved elements in seawater: The influence of pH on concentration ratios. *Geochem. Trans.* **3**, 11–16.

Chen T.-Y., Ling H.-F., Frank M., Zhao K.-D. and Jiang S.-Y. (2011) Zircon effect alone insufficient to generate seawater Nd–Hf isotope relationships. *Geochem. Geophys. Geosyst.* **12**, Q05003. http://dx.doi.org/10.1029/2010gc003363.

Chen T.-Y., Li G., Frank M. and Ling H.-F. (2013) Hafnium isotope fractionation during continental weathering: Implications for the generation of the seawater Nd–Hf isotope relationship. *Geophys. Res. Lett.* **40**, 916–920. http://dx.doi.org/10.1002/grl.50217.

Chu N.-C., Taylor R. N., Chavagnac V., Nesbitt R. W., Boella R. M., Milton J. A., German C. R., Bayon G. and Burton K. (2002) Hf isotope ratio analysis using multi-collector inductively coupled plasma mass spectrometry: An evaluation of isobaric interference corrections. *J. Anal. At. Spectrom.* **17**, 1567–1574.

Dahlqvist R., Andersson P. S. and Ingri J. (2005) The concentration and isotopic composition of diffusible Nd in fresh and marine waters. *Earth Planet. Sci. Lett.* **233**, 9–16.

Dalsgaard T., De Brabandere L. and Hall P. O. J. (2013) Denitrification in the water column of the central Baltic Sea. *Geochim. Cosmochim. Acta* **106**, 247–260.

David K., Frank M., O'Nions R. K., Belshaw N. S. and Arden J. W. (2001) The Hf isotope composition of global seawater and the evolution of Hf isotopes in the deep Pacific Ocean from Fe–Mn crusts. *Chem. Geol.* **178**, 23–42.

Erel Y., Blum J. D., Roueff E. and Ganor J. (2004) Lead and strontium isotopes as monitors of experimental granitoid mineral dissolution. *Geochim. Cosmochim. Acta* **68**, 4649–4663.

Feistel R., Nausch G., Matthäus W. and Hagen E. (2003) Temporal and spatial evolution of the Baltic deep water renewal in spring 2003. *Oceanologia* **45**, 623–642.

Firdaus M. L., Minami T., Norisuye K. and Sohrin Y. (2011) Strong elemental fractionation of Zr–Hf and Nb–Ta across the Pacific Ocean. *Nat. Geosci.* **4**, 227–230.

Frank M. (2002) Radiogenic isotopes: Tracers of past ocean circulation and erosional input. *Rev. Geophys.* **40**, 1001. http://dx.doi.org/10.1029/2000RG000094.

Gaál G. and Gorbatschev R. (1987) An Outline of the precambrian evolution of the baltic shield. *Precambrian Res.* **35**, 15–52.

German C. R., Klinkhammer G. P., Edmond J. M., Mitra A. and Elderfield H. (1990) Hydrothermal scavenging of rare-earth elements in the ocean. *Nature* **345**, 516–518.

German C. R., Holliday B. P. and Elderfield H. (1991) Redox cycling of rare-earth elements in the suboxic zone of the black-sea. *Geochim. Cosmochim. Acta* **55**, 3553–3558.

Godfrey L. V., White W. M. and Salters V. J. M. (1996) Dissolved zirconium and hafnium distributions across a shelf break in the northeastern Atlantic Ocean. *Geochim. Cosmochim. Acta* **60**, 3995–4006.

Godfrey L. V., Field M. P. and Sherrell R. M. (2008) Estuarine distributions of Zr, Hf, and Ag in the Hudson River and the implications for their continental and anthropogenic sources to seawater. *Geochem. Geophys. Geosyst.* **9**, Q12007. http://dx.doi.org/10.1029/2008gc002123.

Godfrey L. V., Zimmermann B., Lee D. C., King R. L., Vervoort J. D., Sherrell R. M. and Halliday A. N. (2009) Hafnium and neodymium isotope variations in NE Atlantic seawater. *Geochem. Geophys. Geosyst.* **10**, Q08015. http://dx.doi.org/10.1029/2009GC002508.

Goldstein S. L., Hemming S. R., Heinrich D. H. and Karl K. T. (2003) Long-lived isotopic tracers in oceanography, paleoceanography, and ice-sheet dynamics. In *Treatise on Geochemistry*. Pergamon, Oxford.

Graham P. L. (2000) *Large-scale hydrologic modeling in the Baltic basin*. KTH.

Halliday A. N., Davidson J. P., Holden P., Owen R. M. and Olivarez A. M. (1992) Metalliferous sediments and the scavenging residence time of Nd near hydrothermal vents. *Geophys. Res. Lett.* **19**, 761–764.

Hansson M., Axe P., and Andersson L. (2009) Extent of anoxia and hypoxia in the Baltic Sea, 1960–2009, SMHI Report Mo2009-214. Available online at <http://www.smhi.se/polopoly_fs/1.10354!Oxygen_timeseries_1960_2009.pdf>.

Harlavan Y. and Erel Y. (2002) The release of Pb and REE from granitoids by the dissolution of accessory phases. *Geochim. Cosmochim. Acta* **66**, 837–848.

Harlavan Y., Erel Y. and Blum J. D. (1998) Systematic changes in lead isotopic composition with soil age in glacial granitic terrains. *Geochim. Cosmochim. Acta* **62**, 33–46.

Ingri J., Widerlund A., Land M., Gustafsson Ö., Andersson P. and Öhlander B. (2000) Temporal variations in the fractionation of the rare earth elements in a boreal river; the role of colloidal particles. *Chem. Geol.* **166**, 23–45.

Jacobsen S. B. and Wasserburg G. J. (1980) Sm–Nd isotopic evolution of chondrites. *Earth Planet. Sci. Lett.* **50**, 139–155.

Kuhlmann G., de Boer P. L., Pedersen R. B. and Wong T. E. (2004) Provenance of Pliocene sediments and paleoenvironmental changes in the southern North Sea region using Samarium–Neodymium (Sm/Nd) provenance ages and clay mineralogy. *Sediment. Geol.* **171**, 205–226.

Lacan F. and Jeandel C. (2001) Tracing papua new guinea imprint on the central equatorial pacific ocean using neodymium isotopic compositions and rare earth element patterns. *Earth Planet. Sci. Lett.* **186**, 497–512.

Lacan F. and Jeandel C. (2005) Neodymium isotopes as a new tool for quantifying exchange fluxes at the continent–ocean interface. *Earth Planet. Sci. Lett.* **232**, 245–257.

Lawrence M. G. and Kamber B. S. (2006) The behaviour of the rare earth elements during estuarine mixing – Revisited. *Mar. Chem.* **100**, 147–161.

Lee D. C., Halliday A. N., Hein J. R., Burton K. W., Christensen J. N. and Gunther D. (1999) Hafnium isotope stratigraphy of ferromanganese crusts. *Science* **285**, 1052–1054.

Lundqvist J. (1986) Late Weichselian glaciation and deglaciation in Scandinavia. *Quaternary Sci. Rev.* **5**, 269–292.

Mansfeld J. (2001) Age and epsilon(Nd) constraints on the Palaeoproterozoic tectonic evolution in the Baltic-Sea region. *Tectonophysics* **339**, 135–151.

Matthäus W., Nehring D., Feistel R., Nausch G., Mohrholz V. and Lass H.-U. (2008) The inflow of highly saline water into the Baltic Sea. In *State and Evolution of the Baltic Sea, 1952–2005, edited*. John Wiley & Sons Inc., pp. 265–309.

Meier H. E. M. (2007) Modeling the pathways and ages of inflowing salt- and freshwater in the Baltic Sea. *Estuar. Coast. Shelf S.* **74**, 610–627.

Neretin L. N., Pohl C., Jost G., Leipe T. and Pollehne F. (2003) Manganese cycling in the Gotland Deep, Baltic Sea. *Mar. Chem.* **82**, 125–143.

Nowell G. M., Kempton P. D., Noble S. R., Fitton J. G., Saunders A. D., Mahoney J. J. and Taylor R. N. (1998) High precision Hf isotope measurements of MORB and OIB by thermal ionisation mass spectrometry: Insights into the depleted mantle. *Chem. Geol.* **149**, 211–233.

Nozaki Y. and Alibo D. S. (2003) Importance of vertical geochemical processes in controlling the oceanic profiles of dissolved rare earth elements in the northeastern Indian Ocean. *Earth Planet. Sci. Lett.* **205**, 155–172.

Öhlander B., Ingri J., Land M. and Schoberg H. (2000) Change of Sm–Nd isotope composition during weathering of till. *Geochim. Cosmochim. Acta* **64**, 813–820.

Oka A., Hasumi H., Obata H., Gamo T. and Yamanaka Y. (2009) Study on vertical profiles of rare earth elements by using an ocean general circulation model. *Global Biogeochem. Cycles* **23**, GB4025. http://dx.doi.org/10.1029/2008GB003353.

Patchett P. J., White W. M., Feldmann H., Kielinczuk S. and Hofmann A. W. (1984) Hafnium rare-earth element fractionation in the sedimentary system and crustal recycling into the earths mantle. *Earth Planet. Sci. Lett.* **69**, 365–378.

Piotrowski J. A. (1997) Subglacial hydrology in north-western Germany during the last glaciation: Groundwater flow, tunnel valleys and hydrological cycles. *Quaternary Sci. Rev.* **16**, 169–185.

Piotrowski A. M., Lee D. C., Christensen J. N., Burton K. W., Halliday A. N., Hein J. R. and Gunther D. (2000) Changes in erosion and ocean circulation recorded in the Hf isotopic compositions of North Atlantic and Indian Ocean ferromanganese crusts. *Earth Planet. Sci. Lett.* **181**, 315–325.

Plieth W. (2008) 3 – Electrode potentials. In *Electrochemistry for Materials Science*. Elsevier, Amsterdam.

Pohl C. and Hennings U. (2008) Trace metals in Baltic Seawater. In *State and Evolution of the Baltic Sea, 1952–2005, edited*. John Wiley & Sons Inc., pp. 367–393.

Pohl C. and Fernández-Otero E. (2012) Iron distribution and speciation in oxic and anoxic waters of the Baltic Sea. *Mar. Chem.* **145–147**, 1–15.

Pohl C. and Hennings U. (2005) The coupling of long-term trace metal trends to internal trace metal fluxes at the oxic–anoxic interface in the Gotland Basin (57°19,20′ N; 20°03,00′ E) Baltic Sea. *J. Mar. Syst.* **56**, 207–225.

Pohl C., Loffler A. and Hennings U. (2004) A sediment trap flux study for trace metals under seasonal aspects in the stratified Baltic Sea (Gotland Basin; 57°19.20′ N; 20°03.00′ E). *Mar. Chem.* **84**, 143–160.

Reissmann J. H., Burchard H., Feistel R., Hagen E., Lass H. U., Mohrholz V., Nausch G., Umlauf L. and Wieczorek G. (2009) Vertical mixing in the Baltic Sea and consequences for eutrophication – A review. *Prog. Oceanogr.* **82**, 47–80.

Rempfer J., Stocker T. F., Joos F., Dutay J. C. and Siddall M. (2011) Modelling Nd-isotopes with a coarse resolution ocean circulation model: Sensitivities to model parameters and source/sink distributions. *Geochim. Cosmochim. Acta* **75**, 5927–5950.

Rickli J., Frank M. and Halliday A. N. (2009) The hafnium–neodymium isotopic composition of Atlantic seawater. *Earth Planet. Sci. Lett.* **280**, 118–127.

Rickli J., Frank M., Baker A. R., Aciego S., de Souza G., Georg R. B. and Halliday A. N. (2010) Hafnium and neodymium isotopes in surface waters of the eastern Atlantic Ocean: Implications for sources and inputs of trace metals to the ocean. *Geochim. Cosmochim. Acta* **74**, 540–557.

Rickli J., Frank M., Stichel T., Georg R. B., Vance D. and Halliday A. N. (2013) Controls on the incongruent release of hafnium during weathering of metamorphic and sedimentary catchments. *Geochim. Cosmochim. Acta* **101**, 263–284.

Schlitzer, R. (2012) Ocean Data View, <http://odv.awi.de>.

Schneider B., Ceburnis D., Marks R., Munthe J., Petersen G. and Sofiev M. (2000) Atmospheric Pb and Cd input into the Baltic Sea: A new estimate based on measurements. *Mar. Chem.* **71**, 297–307.

Sholkovitz E. R., Shaw T. J. and Schneider D. L. (1992) The geochemistry of rare-earth elements in the seasonally anoxic water column and porewaters of chesapeake bay. *Geochim. Cosmochim. Acta* **56**, 3389–3402.

Sholkovitz E. R., Landing W. M. and Lewis B. L. (1994) Ocean particle chemistry: The fractionation of rare earth elements between suspended particles and seawater. *Geochim. Cosmochim. Acta* **58**, 1567–1579.

Siddall M., Khatiwala S., van de Flierdt T., Jones K., Goldstein S. L., Hemming S. and Anderson R. F. (2008) Towards explaining the Nd paradox using reversible scavenging in an ocean general circulation model. *Earth Planet. Sci. Lett.* **274**, 448–461.

Staubwasser M., Schoenberg R., von Blanckenburg F., Krüger S. and Pohl C. (2013) Isotope fractionation between dissolved and suspended particulate Fe in the oxic and anoxic water column of the Baltic Sea. *Biogeosciences* **10**, 233–245.

Stichel T., Frank M., Rickli J. and Haley B. A. (2012a) The hafnium and neodymium isotope composition of seawater in the Atlantic sector of the Southern Ocean. *Earth Planet. Sci. Lett.* **317–318**, 282–294.

Stichel T., Frank M., Rickli J., Hathorne E. C., Haley B. A., Jeandel C. and Pradoux C. (2012b) Sources and input mechanisms of hafnium and neodymium in surface waters of the Atlantic sector of the Southern Ocean. *Geochim. Cosmochim. Acta* **94**, 22–37.

Tachikawa K., Athias V. and Jeandel C. (2003) Neodymium budget in the modern ocean and paleo-oceanographic implications. *J. Geophys. Res.* **108**, 3254. http://dx.doi.org/10.1029/1999jc000285.

Tanaka T., Togashi S., Kamioka H., Amakawa H., Kagami H., Hamamoto T., Yuhara M., Orihashi Y., Yoneda S., Shimizu H., Kunimaru T., Takahashi K., Yanagi T., Nakano T., Fujimaki H., Shinjo R., Asahara Y., Tanimizu M. and Dragusanu C. (2000) JNdi-1: A neodymium isotopic reference in consistency with LaJolla neodymium. *Chem. Geol.* **168**, 279–281.

Turnewitsch R. and Pohl C. (2010) An estimate of the efficiency of the iron- and manganese-driven dissolved inorganic phosphorus trap at an oxic/euxinic water column redoxcline. *Global Biogeochem. Cycles* **24**, GB4025. http://dx.doi.org/10.1029/2010GB003820.

Ulfsbo A., Hulth S. and Anderson L. G. (2011) PH and biogeochemical processes in the Gotland Basin of the Baltic Sea. *Mar. Chem.* **127**, 20–30.

van de Flierdt T., Frank M., Lee D. C. and Halliday A. N. (2002) Glacial weathering and the hafnium isotope composition of seawater. *Earth Planet. Sci. Lett.* **198**, 167–175.

van de Flierdt T., Frank M., Lee D. C., Halliday A. N., Reynolds B. C. and Hein J. R. (2004) New constraints on the sources and behavior of neodymium and hafnium in seawater from Pacific Ocean ferromanganese crusts. *Geochim. Cosmochim. Acta* **68**, 3827–3843.

Vervoort J. D., Patchett P. J., Blichert-Toft J. and Albarede F. (1999) Relationships between Lu–Hf and Sm–Nd isotopic systems in the global sedimentary system. *Earth Planet. Sci. Lett.* **168**, 79–99.

von Blanckenburg F. (1999) Perspectives: Paleoceanography – Tracing past ocean circulation? *Science* **286**, 1862–1863.

Yakushev E. V., Pollehne F., Jost G., Kuznetso I., Schneider B. and Urnlauf L. (2007) Analysis of the water column oxic/anoxic interface in the Black and Baltic seas with a numerical model. *Mar. Chem.* **107**, 388–410.

Yemenicioglu S., Erdogan S. and Tugrul S. (2006) Distribution of dissolved forms of iron and manganese in the Black Sea. *Deep-Sea Res. Part. II* **53**, 1842–1855.

Zimmermann B., Porcelli D., Frank M., Andersson P. S., Baskaran M., Lee D. C. and Halliday A. N. (2009a) Hafnium isotopes in Arctic Ocean water. *Geochim. Cosmochim. Acta* **73**, 3218–3233.

Zimmermann B., Porcelli D., Frank M., Rickli J., Lee D. C. and Halliday A. N. (2009b) The hafnium isotope composition of Pacific Ocean water. *Geochim. Cosmochim. Acta* **73**, 91–101.

Associate editor: Derek Vance